NANO LETTERS

pubs.acs.org/NanoLett

Electronic Signatures of all Four DNA Nucleosides in a Tunneling Gap

Shuai Chang,[†,‡] Shuo Huang,[†,‡] Jin He,[†] Feng Liang,[†] Peiming Zhang,[†] Shengqing Li,[†] Xiang Chen,[‡] Otto Sankey,[‡] and Stuart Lindsay*[,†,‡,§]

[†]Biodesign Institute, [‡]Department of Physics, and [§]Department of Chemistry and Biochemistry, Arizona State University, Tempe, Arizona 85287

ABSTRACT Nucleosides diffusing through a 2 nm electron-tunneling junction generate current spikes of sub-millisecond duration with a broad distribution of peak currents. This distribution narrows 10-fold when one of the electrodes is functionalized with a reagent that traps nucleosides in a specific orientation with hydrogen bonds. Functionalizing the second electrode reduces contact resistance to the nucleosides, allowing them to be identified via their peak currents according to deoxyadenosine > deoxycytidine > deoxyguanosine > thymidine, in agreement with the order predicted by a density functional calculation.

KEYWORDS DNA sequencing, electron tunneling, DNA nucleosides, hydrogen bonding, molecular recognition

New approaches to DNA sequencing are required to reduce costs and increase the availability of personalized genomics.[1] In addition, long contiguous reads would help to unravel the long-range structure of the genome.[2,3] In contrast to Sanger sequencing and next-generation methods, nanopore sequencing[4] is an enzyme-free technique in which DNA molecules are forced through a tiny aperture using electrophoresis, so that a sequence-reading mechanism could maintain its fidelity over the entire length of a molecule. Ion current that passes through the pore is sensitive to the sequence in the nanopore[5−7] but all of the bases in the nanopore channel contribute to the current blockade[8] as well as those in the region of high field beyond the pore.[9,10] As a consequence, single base resolution has not yet been attained with an ion current readout. Lee and Thundat proposed that electron tunneling across a DNA molecule might be localized enough to sense and identify single nucleotides,[11] a conjecture supported by the calculations of Zwolak and Di Ventra.[12] Further calculations show that thermal motion of molecules in the gap broadens the distribution of tunnel currents,[13,14] reducing selectivity substantially. The range of orientations of molecules in a tunnel gap can be greatly reduced by using chemical bonds to tether it to the readout electrodes;[15] however, the use of strong bonds is clearly not an option for DNA sequencing where the contact to the electrodes must slide from one nucleotide to the next rapidly. Ohshiro and Umezawa demonstrated that hydrogen bonds can be used to provide chemical contrast in scanning tunneling microscope images[16] suggesting that these weaker bonds can serve as "sliding contacts" to single molecules. We have used chemical reagents that hydrogen bond to DNA[17] and the nucleosides[18] to measure conductances for single nucleosides bound to an electrode, finding values that are in reasonable agreement with density functional calculations.[19,20] Here, we report measurements of the current signals generated as free nucleosides diffuse into a tunnel junction in which both electrodes are functionalized with a reagent that presents a hydrogen bond donor and acceptor to the nucleosides (Figure 1A). This functionalization serves to both limit the range of molecular orientations in the tunnel gap and reduce the contact resistance, increasing the selectivity of the tunneling signal, so that a direct readout may be possible with a few repeated reads.

In order to reduce complications associated with electrochemical leakage, we operated in an organic solvent (1,2,4-trichlorobenzene, TCB) and the OH groups of the deoxyribose ring of all four nucleosides were protected with *tert*-butyldimethylsilyl (TBDMS) to improve their solubility. Gold electrodes were functionalized with 4-mercaptobenzoic acid, forming monolayers with the benzoic acid moiety exposed to solvent.[21,22] In nonpolar solvent, the benzoic acid is neutral, the O−H group acting as a hydrogen bond donor and the carbonyl oxygen acting as a hydrogen bond acceptor.[23] Hydrogen bond configurations for trapping all four nucleosides are shown in panels D−G in Figure 1. These are the optimized configurations, assuming that our estimate of the tunnel gap is correct. Synthesis, preparation, and characterization of all reagents, probes, and surfaces are described in the Supporting Information.

We carried out tunneling measurements on a PicoSPM scanning probe microscope (Agilent, Chandler) interfaced to a digital oscilloscope. When both the probe and a gold (111) substrate were functionalized with 4-mercaptobenzoic acid, the tunneling background signal in TCB was relatively noise free for set-points currents, I_{bl} of up to 10 pA at 0.5 V bias, a conductance of 20 pS (Figure 1B and Figure S2 in

* To whom correspondence should be addressed, Stuart.Lindsay@asu.edu.
Received for review: 01/13/2010
Published on Web: 02/08/2010

DOI: 10.1021/nl1001185 | *Nano Lett.* **2010,** *10,* 1070–1075

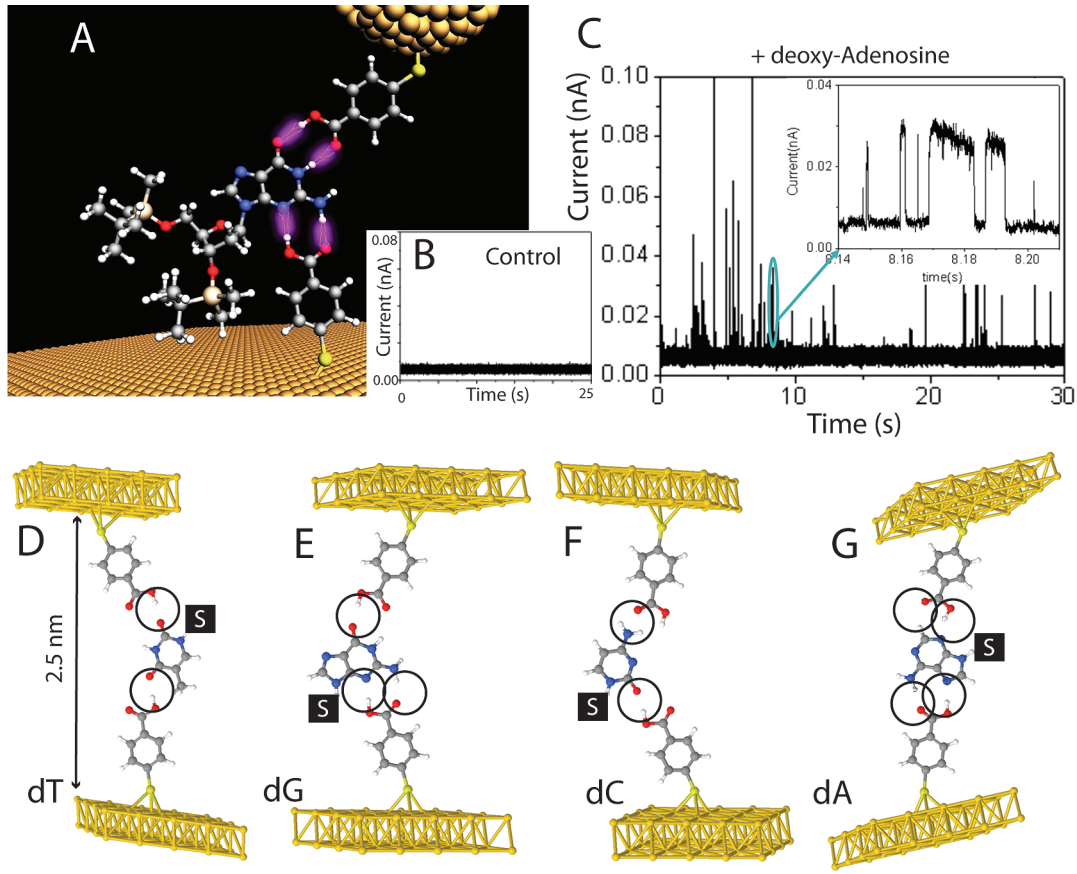

FIGURE 1. Tunneling measurements with functionalized electrodes. (A) A gold probe and a gold substrate are functionalized with a monolayer of 4-mercaptobenzoic acid, and the size of the gap between two electrodes maintained under servo control at a value such that the two monolayers do not interact with one another, resulting in a tunnel current signal that is free of spikes (B). When a solution of nucleosides is introduced, current spikes appear, as shown here for[24] 0.7 μM deoxyadenine in trichlorbenzene with a baseline tunneling current of 6 pA at a bias of 0.5 V (C). Hydrogen-bonding schemes for all four nucleosides are shown in panels D−F. "S" represents the modified deoxyribose sugar (Supporting Information) and the hydrogen bonds are circled.

Supporting Information). A nucleoside solution was placed in the liquid cell, and after the polarization current had fallen to a small value (Supporting Information) we re-engaged the probe at a tunnel current level that had previously given a low-noise background signal. Current spikes were immediately obvious in the tunneling signal (Figure 1C and Figure S3 in Supporting Information). Because neither the surface concentrations of nucleosides nor the efficiency of molecular capture in the gap is known a priori, we adjusted the concentrations of the nucleoside solutions to give approximately equal "spike rates" in the tunnel gap (Table 1 and Supporting Information). Many of the "spikes" showed the two-level "telegraph noise" characteristic[19] of binding and unbinding of a single molecule in the gap (insets, Figure 1C, Figure S3 in Supporting Information). The STM servo gains were set so that only spikes of the longest duration were affected by the action of the current-control servo (Figure S4 in Supporting Information).

We generated distributions of the peak currents using a custom program to analyze the height of the spikes. The program captures signals two standard deviations above the noise on the baseline, and also rejects data of only one or two points in time (i.e., up to 40 μs duration). The effect of the choice of filtering parameters on the measured distribution is discussed in the Supporting Information (Figures S5 and S14−15). Figure 2 shows how these measured distributions are affected by functionalization of the electrodes. Distributions recorded with bare electrodes are shown in panels A and C of Figure 2. In order to record signals with bare electrodes, we had to reduce the tunneling gap a little

TABLE 1. Measured and Calculated Conductances in a Functionalized Tunnel Junction at I_{bl} = 6 pA, V = 0.5 V[a]

	dT	dG	dC	dA
measured G (pS)	13.6 ± 0.3	18.6 ± 0.9	25.3 ± 2.5	33 ± 1.9
calculated G (pS)	0.04	0.12	0.51	1.05
read rate (s^{-1})	7.1 ± 1.4	5.5 ± 1.1	5.5 ± 1.1	6.6 ± 1.3

[a] Measured values are the average of three independent runs (errors are ±1 sd). Calculated conductances are for the structures shown in Figure 1D−G. Read rate is based on counts acquired in a 180 s period for nucleoside concentrations between 0.8 and 4.3 μM (Supporting Information). The disparity in the range of values between theory and experiment may reflect neglect of a background contribution via solvent-mediated tunneling into a molecule bound at one electrode.[27] Absolute values will be affected by inaccuracies in the estimate of the gap size.

DOI: 10.1021/nl1001185 | *Nano Lett.* **2010,** *10,* 1070–1075

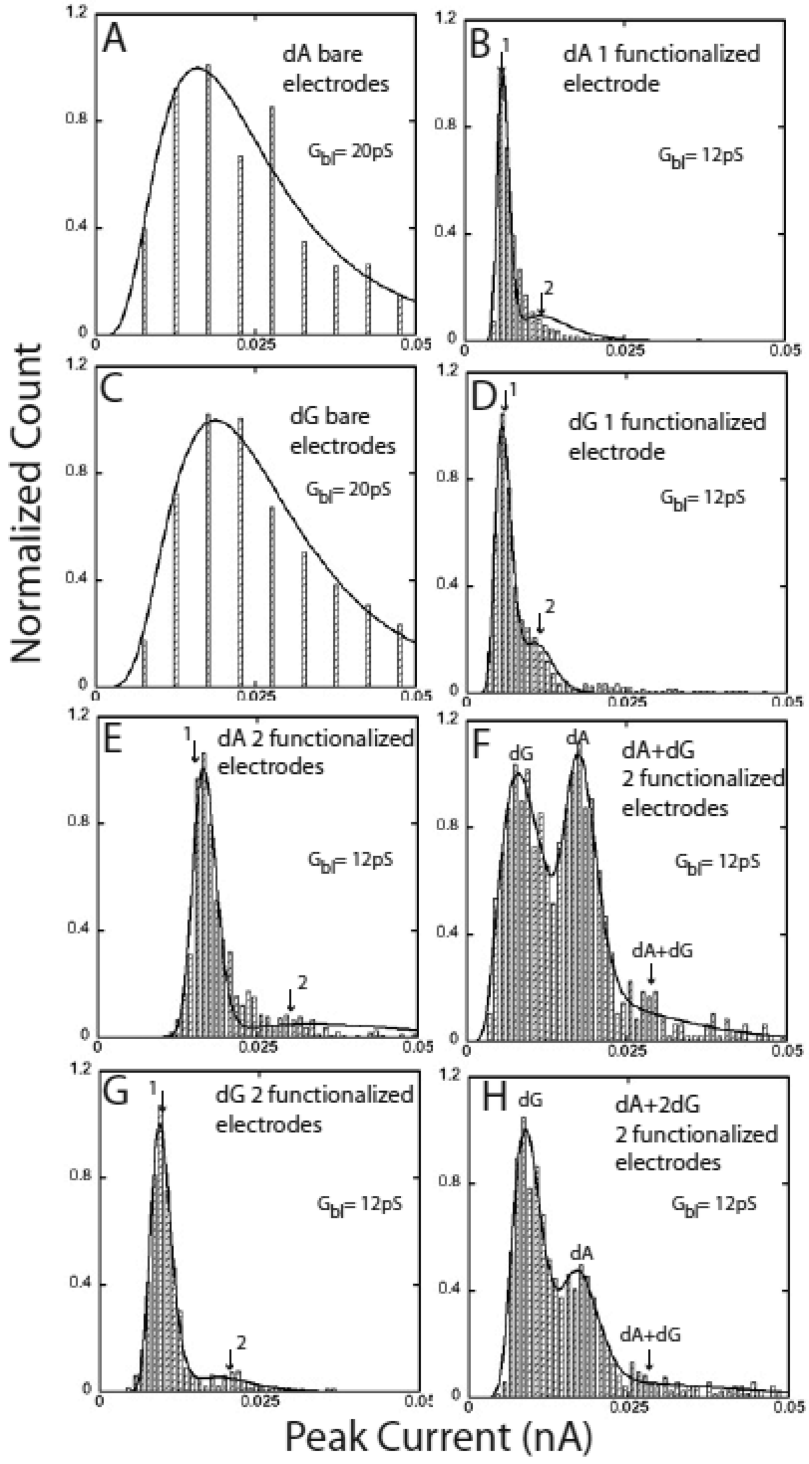

FIGURE 2. Effect of electrode functionalization on the distribution of current spikes for purines. Bare electrodes (A, dA; C, dG) give broad distributions (gap conductance 20 pS, 0.7 μM dA, 2.9 μM dG in TCB). Fits are Gaussian in the log of the current (Figures S6−8, Supporting Information). Distributions narrow 10-fold when one electrode is functionalized with 4-mercaptobenzoic acid (B, dA; D, dG) (gap conductance 12 pS, $I_{bl} = 6$ pA, $V = 0.5$ V). Fits are to two Gaussians in the log of the current with a peak at i_0 ("1") and a second at 2 i_0 ("2") (eq S3). $i_0 =$ 5.9 pA for dA and 5.6 pA for dG. When both electrodes are functionalized (E, dA; G, dG) the peak currents are clearly different ($i_0 = 9.4$ pA for dG, $i_0 = 16.5$ pA for dA). (F) Distribution for a mixture of dA and dG. The assignment of the higher peak to dA is confirmed by the distribution measured with a reduced concentration of dA (H). The high current tail in (F) and (H) is consistent with a small number of two molecule (dA+dG) reads. Distributions of the spike widths are given in Figure S16 (Supporting Information).

by operating at a conductance of 20 pS. Even at this smaller gap, reads with bare electrodes on the pyrimidine nucleosides were much less frequent than reads on purine nucleosides (Figure S6 and Table S2 in Supporting Information).

DOI: 10.1021/nl1001185 | *Nano Lett.* **2010,** *10,* 1070–1075

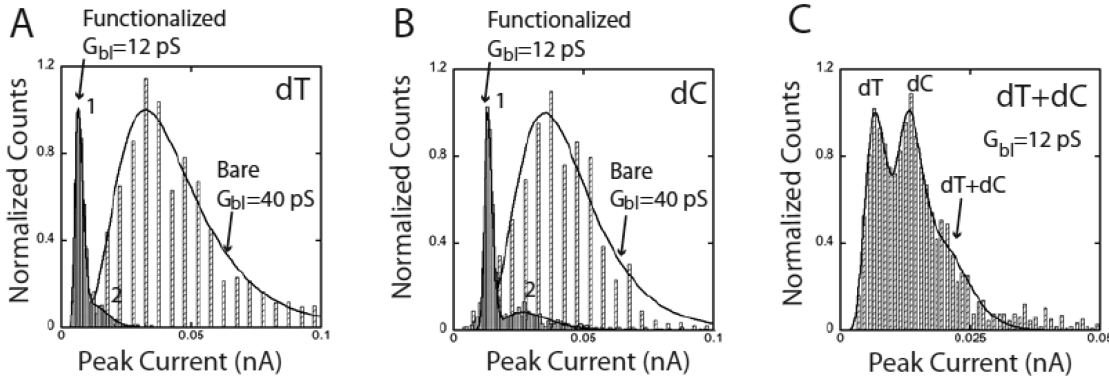

FIGURE 3. Effect of electrode functionalization for pyrimidine reads. For bare reads (broad distributions in A and B) G_{bl} was increased to 40 pS to increase the count rate. The narrow distributions in A and B are taken with both electrodes functionalized and yield $i_0 = 6.7$ pA for dT and 13.3 pA for dC ($G_{bl} = 12$ pS, $I_{bl} = 6$ pA, $V = 0.5$ V). In a mixed solution, (C) the dT peak occurs at 8 pA and the dC peak occurs at 13.4 pA, an assignment verified by measuring a mixture with half the concentration of dT (Figure S9 in Supporting Information).

The measured current distributions were fitted quite well by a Gaussian distribution of the logarithm of the currents (solid lines) as described in the Supporting Information and Figures S6−S8. The fitted peak currents differ for these two nucleosides (15.9 ± 0.4 pA for dA and 18.7 ± 0.2 pA for dG) but the difference (2.8 pA) is less than the width of the distribution on the high current side (~15 pA). When measurements are repeated with a functionalized substrate and a bare gold probe at an increased gap (corresponding to 12 pS) the distribution of measured currents narrows by an order of magnitude (Figure 2B, dA; Figure 2D, dG) but the peak currents are not significantly different. The distribution of spike lifetimes is quite similar both for bare electrodes and for one functionalized electrode (Figure S16, Supporting Information). Thus, it appears likely that the spikes observed with bare electrodes correspond to transiently bound states of the nucleosides also. If this is the case, then the narrowing observed with a functionalized electrode must be a consequence of a reduction in the number of types of bound states in the tunnel gap. When both probe and substrate are functionalized (Figure 2E, dA; Figure 2G, dG), the peak current for dA is clearly higher than the peak current for dG. Thus distinctive signals can be generated when both electrodes are functionalized, but do they originate with single nucleosides? The "telegraph noise" signals are characteristic of single-molecule reads, and the small size of the peaks assigned to two-molecule reads ("2" in Figure 2, panels B, D, E, and G) suggests that reads of more than one molecule at a time are infrequent. However, electrochemical leakage currents can introduce current errors that depend on the nucleoside (Supporting Information) so the measured current may not be generated from single molecule currents alone. A better test of the fidelity of tunneling reads can be carried out using mixtures of two nucleosides so that any errors owing to an electrochemical background are present in both sets of signals. Figure 2F shows the current distribution obtained with a mix of dA and dG. The higher current peak is at essentially the same current as recorded for dA alone, and thus should count the dA molecules in this mixture. This assignment is confirmed by halving the concentration of dA in solution (Figure 2H).[24] Most of the data in this panel were well fitted assuming single molecule reads with only 5% of the reads consistent with both dA and dG in the gap at the same time ("dA+dG", Figure 2F).

The same types of features are observed for dC and dT (Figure 3 and Figure S16) but the data for a bare gap and bare substrate had to be collected at a yet larger tunnel current (20pA, corresponding to 40 pS) in order to acquire a significant number of reads for the (smaller-sized) pyrimidine nucleosides (Figure S7 in Supporting Information). dC and dT are also clearly separated in a mixed sample when read with probes that are functionalized (Figure 3C and Figure S9). We did not carry out experiments with A:T and G:C mixtures because control of surface concentrations is complicated by competition from Watson−Crick base pairing, a complication that should be minimized in a nanopore reader.

At a given bias, the absolute value of peak current is directly proportional to the baseline conductance of the gap (Figure 4A); i.e., it increases exponentially as the gap is decreased, similar to what has been reported for other hydrogen-bonded systems in large tunnel gaps.[19] We found evidence of an interesting dependence of the peak currents on bias at a fixed gap size (i.e., gap conductance) (Figure S10 in Supporting Information) indicating the possibility of a nonlinear current−voltage dependence for molecules bound to both electrodes. The read frequency also increased as the gap was narrowed (Figure S11 in Supporting Information). On the other hand, the fraction of multimolecule reads increased rapidly in smaller gaps (Figure 4A and Figure S12) so 12 pS appears to be an optimal value for the baseline conductance at a bias of 0.5 V.

Values for the peak currents measured at $I_{bl} = 6$ pA, $V =$ 0.5 V are summarized by the cross-hatched bars in Figure 4B. These are the results of three different runs (one carried out, from sample preparation to data analysis, by a different team) on each of the four nucleosides. The peaks for each nucleoside are separated by an amount comparable to the

DOI: 10.1021/nl1001185 | *Nano Lett.* **2010,** *10,* 1070–1075

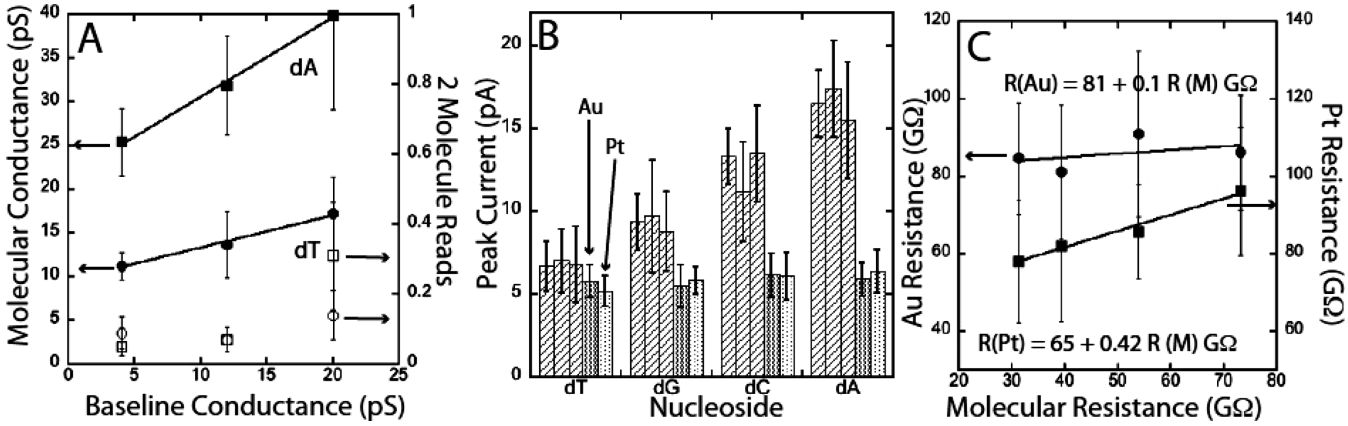

FIGURE 4. Summary of the reads. (A) The measured molecular conductance increases linearly with G_{bl} (black circles dT, black squares dA, error bars are ±HWHH). The number of two molecule reads (open circles, dT, open squares, dA) increases at $G_{bl} = 20$ pS, and the read rate is substantially reduced at $G_{bl} = 4$ pS (Supporting Information). (B) Peak currents measured in three independent runs for the four nucleosides (cross hatched bars). Error bars represent the HWHH of the current distributions. Reads for a functionalized surface and a bare Pt (light shaded bars) and bare Au (dark shaded bars) probe are relatively insensitive to the identity of the nucleoside, as shown quantitatively in (C) where the junction resistance is plotted vs the molecular resistance determined with two functionalized probes.

width of the distribution, allowing the fraction that are single-molecule reads with two "good" contacts to identify the base with $p \geq 0.6$ (Figure S13 in Supporting Information).

We also recorded data with a functionalized substrate and a bare Au (dark shaded bars) or bare Pt (light shaded bars) probe. The peak currents change little from nucleoside to nucleoside, an expected consequence of the resistance, R_c, associated with bare contacts[15] although the lack of selectivity is not accounted for by contact resistance alone. If we assume that reads with two functionalized probes determine a resistance for a single molecule, R_m, then the resistance of a junction with one bare electrode should be given by $R_j = R_c + R_m$. Figure 4C shows that the signal with one bare gold electrode is insensitive to the molecular resistance, while a bare Pt electrode is about half as sensitive as the simple "resistors in series" model predicts, probably reflecting the way in which binding to the electrodes affects the position of molecular states.[25]

At 12 pS conductance, we estimate the gap to be about 2.5 nm, using $G = G_0 \exp(-\beta x)$ where G_0 is the quantum of conductance (77 μS) and $\beta = 6.4$ nm^{-1}.[26] Panels D–G of Figure 1 show what we believe to be the most likely hydrogen bonded (energy-minimized) structures for the four nucleosides in a gap with both electrodes functionalized. We carried out density functional calculations of the conductance of these four molecular junctions (Supporting Information), and the predicted conductances are listed below the measured values in Table 1. The predicted order of conductance agrees with experiment, though the absolute values are significantly lower, possibly because of an overestimate of the size of the tunnel gap.[27]

The present work shows that the two major impediments to sequence readouts by tunneling—a wide range of molecular orientations and a large contact resistance—can be overcome using functionalized electrodes.[28] Overlap between peaks limits the probability of a correct read to ≥0.6. The successful read rate is further lowered by the presence of a significant fraction of "single contact" reads (i.e., peaks that appear at the same place as found with just one functionalized electrodes). These can amount to about half the total reads, depending on the probe and the point on the substrate that is sampled (Figures S14–15 in Supporting Information). The solution concentrations required to get approximately equal read rates differed by a maximum factor of 6 (Supporting Information) so the reading efficiencies for each base are unlikely to differ by a large amount. These efficiencies will be better measured once a recognition molecule is developed for reads in aqueous electrolytes using oligonucleotide targets. The recent introduction of a naturally conductive nanopore[29] might facilitate the integration of a tunneling readout into a nanpore device.

Acknowledgment. This work was supported by a grant from the Sequencing Technology Program of the National Human Genome Research Institute (HG004378). We thank Michael Tuchband for assistance with sample preparation, Hao Liu for artwork, and Predrag Krstic for comments on the manuscript.

Supporting Information Available. Synthesis and characterization of materials, preparation and characterization of probes and surfaces, background tunneling signals, polarization currents and electrochemical leakage, examples of raw data for dT, dG, and dC, STM servo gain, automatic peak detection, data obtained with bare electrodes, data for mixed solutions of nucleosides, bias dependence of peak current and measurements at a fixed gap, read frequency as a function of gap size, multimolecule reads in small gaps, probability of a correct identification from one read, time discrimination and lifetime distributions, and calculations of conductances for hydrogen bonded complexes. This material is available free of charge via the Internet at http://pubs.acs.org.

DOI: 10.1021/nl1001185 | *Nano Lett.* **2010,** *10,* 1070–1075

REFERENCES AND NOTES

(1) Zwolak, M.; Di Ventra, M. *Rev. Mod. Phys.* **2008**, *80*, 141–165.
(2) Pennish, E. *Science* **2007**, *318*, 1842–1843.
(3) Sharp, A. J.; Cheng, Z. C.; Eichler, E. E. *Annu. Rev. Genomics Hum. Genet.* **2006**, *ARI*, 407–442.
(4) Branton, D.; Deamer, D.; Marziali, A.; Bayley, H.; Benner, S. A.; Butler, T.; Di Ventra, M.; Garaj, S.; Hibbs, A.; Huang, X.; Jovanovich, S. B.; Krstic, P. S.; Lindsay, S.; Ling, X. S.; Mastrangelo, C. H.; Meller, A.; Oliver, J. S.; Pershin, Y. V.; Ramsey, J. M.; Riehn, R.; Soni, G. V.; Tabard-Cossa, V.; Wanunu, M.; Wiggin, M.; Schloss, J. *Nat. Biotechnol.* **2008**, *26*, 1146–1153.
(5) Akeson, M.; Branton, D.; Kasianowicz, J. J.; Brandin, E. *Biophys. J.* **1999**, *77*, 3227–3233.
(6) Meller, A.; Nivon, L.; Brandin, E.; Golovchenko, J.; Branton, D. *Proc. Natl. Acad. Sci. U.S.A.* **2000**, *97*, 1079–1084.
(7) Ashkenasy, N.; Sanchez-Quesada, J.; Bayley, H.; Ghadiri, M. R. *Angew. Chem., Int. Ed.* **2005**, *44*, 1401–1404.
(8) Meller, A.; Nivon, L.; Branton, D. *Phys. Rev. Lett.* **2001**, *86*, 3435–3438.
(9) Aksimentiev, A.; Heng, J. B.; Timp, G.; Schulten, K. *Biophys. J.* **2004**, *87* (3), 2086–2097.
(10) Muthukumar, M.; Kong, C. Y. *Proc. Natl. Acad. Sci. U.S.A.* **2006**, *103*, 5273–5278.
(11) Lee, J. W.; Thundat, T. DNA and RNA sequencing by nanoscale reading through programmable electrophoresis and nanoelectrode-gated tunneling and dielectric detection US Patent 6,905,586, June 14, 2005.
(12) Zwolak, M.; Di Ventra, M. *Nano Lett.* **2005**, *5*, 421–424.
(13) Lagerqvist, J.; Zwolak, M.; Di Ventra, M. *Biophys. J.* **2007**, *93*, 2384–2390.
(14) Zikic, R.; Kristic, P. S.; Zhang, X.-G.; Fuentes-Cabrera, M.; Wells, J.; Zhao, X. *Phys. Rev. E* **2006**, *74*, 011919 1-9.
(15) Cui, X. D.; Primak, A.; Zarate, X.; Tomfohr, J.; Sankey, O. F.; Moore, A. L.; Moore, T. A.; Gust, D.; Harris, G.; Lindsay, S. M. *Science* **2001**, *294*, 571–574.
(16) Ohshiro, T.; Umezawa, Y. *Proc. Natl. Acad. Sci. U.S.A.* **2006**, *103*, 10–14.
(17) He, J.; Lin, L.; Liu, H.; Zhang, P.; Lee, M.; Sankey, O. F.; Lindsay, S. M. *Nanotechnology* **2009**, *20*, 075102−075110.
(18) Chang, S.; He, J.; Kibel, A.; Lee, M.; Sankey, O. F.; Zhang, P.; Lindsay, S. M. *Nat. Nanotechnol.* **2009**, *4*, 297–301.
(19) Chang, S.; He, J.; Lin, L.; Zhang, P.; Liang, F.; Young, M.; Huang, S.; Lindsay, S. *Nanotechnology* **2009**, *20*, 075102−075110.
(20) Lee, M. H.; Sankey, O. F. *Phys. Rev.E* **2009**, *79*, 051911 1−10.
(21) Schäfer, A. H.; Seidel, C.; Chi, L.; Fuchs, H. *Adv. Mater.* **1998**, *10*, 839–842.
(22) Creager, S. E.; Steiger, C. M. *Langmuir* **1995**, *11*, 1852–1854.
(23) Jeffrey, G. A., *An Introduction to Hydrogen Bonding*. Oxford University Press: Oxford, 1997.
(24) Surface concentrations are unknown a priori and dependent on competition between nucleosides for surface binding sites and the different dissociation rates back into solution so absolute signal rates cannot be interpreted in terms of concentrations quantitatively.
(25) Meunier, V.; Kristic, P. S. *J. Chem. Phys.* **2008**, *128*, 041103−1−4.
(26) He, J.; Lin, L.; Zhang, P.; Lindsay, S. M. *Nano Lett.* **2007**, *7*, 3854–3858.
(27) Lifetime data (Figure S16 in Supporting Information) for dT show little change when both electrodes are functionalized, so the dT spikes may represent solvent-mediated tunneling at one electrode. Since solvent molcules are not included in the simulations, this additional tunneling contribution is absent from the predictions. Accordingly, a constant background should be added to each of the predicted currents, which would diminish the discrepancy between the range of predicted and measured currents.
(28) Bare-electrode reads show some sensitivity to the identity of the nucleosides via differences in the widths of the distribution (with purines generating more current than pyrimidines, Table S2 in Supporting Information).
(29) Liu, H.; He, J.; Tang, J.; Liu, H.; Pang, P.; Cao, D.; Kristic, P. S.; Joseph, S.; Lindsay, S.; Nuckolls, C. *Science* **2010**, *327*, 64–67.

DOI: 10.1021/nl1001185 | *Nano Lett.* **2010,** *10,* 1070–1075